Influence of intrapulse Raman scattering on stationary pulses in the presence of linear and nonlinear gain as well as spectral filtering

Ivan M. Uzunov,[1,*] Zhivko D. Georgiev,[2,†] and Todor N. Arabadzhiev[1,‡]

[1]*Department of Applied Physics, Technical University Sofia, 8 Kliment Ohridski Boulevard, Sofia 1000, Bulgaria*

[2]*Department of Theoretical Electrical Egineering, Technical University Sofia, 8 Kliment Ohridski Boulevard, Sofia 1000, Bulgaria*

(Received 14 July 2014; published 8 October 2014)

We examine numerically the influence of intrapulse Raman scattering (IRS) on the stable stationary pulses in the presence of constant linear and nonlinear gain as well as spectral filtering. Numerical results show that the small change of the value of the parameter describing IRS leads to qualitatively different behavior of the evolution of pulse amplitudes. We prove that the strong dependence of the pulse dynamics on the parameter describing IRS is related to the existence of the Poincaré-Andronov-Hopf bifurcation and the appearance of the unstable limit cycle.

DOI: 10.1103/PhysRevE.90.042906 PACS number(s): 05.45.−a, 42.81.Dp

I. INTRODUCTION

As is well known, the complex cubic-quintic Ginzburg-Landau equation (CCQGLE) has been used to describe a variety of phenomena including second-order phase transitions, superconductivity, superfluidity, Bose-Einstein condensation, liquid crystals, and string theory [1,2]. In optics the CCQGLE can model, for example, soliton transmission lines [3,4] as well as passively-mode-locked laser systems [5,6]. The CCQGLE has exact chirped solitary-wave solutions [7–10]. Numerical solutions of the CCQGLE could be divided into two groups: localized fixed-shape solutions and localized pulsating solutions. Localized fixed-shape solutions are the stable stationary pulses, the composite pulses, and the moving pulses [11]. Localized pulsating solutions can be plain pulsating, creeping, snaking, and erupting solutions [12,13]. Chaotic pulsating and period-doubling solutions were observed in [14] (for reviews see [15]). An analysis of the observed solutions of the CCQGLE using the variational method has been performed in [16,17]. It was found that the corresponding Euler-Lagrange equations have periodic, quasiperiodic, and chaotic attractors, which have been related to numerically observed solutions of the CCQGLE [16,17].

The influence of higher-order effects [the third order of dispersion, intrapulse Raman scattering (IRS), and the self-steeping effect (for detailed description of these effects see [18–20])] on the fiber laser operation or, in other words, the influence of higher-order effects on the stable stationary solutions of the CCQGLE, has been studied in [21]. It was shown that narrow-band filtering and nonlinear gain can be used to control the self-frequency shift due to the IRS of ultrashort optical solitons in fiber-optic systems [22]. The role of nonlinear gain is to give an effective gain to the soliton and suppression to the noise or to reduce the background instability [22]. The existence of the exact chirped solitary solution of this generalized CCQGLE that includes the higher-order effects was reported in [23].

The influence of the different higher-order effects as well as their different combinations on the dynamics of the localized pulsating solutions has been numerically studied (see [24,25] and references therein). A strong impact of higher-order effects on the localized pulsating solutions was found. In particular, it was shown that any of the localized pulsating solutions under the combined influence of all higher-order effects can be transformed in fixed-shape solutions for a certain range of parameter values [24].

In this paper we present a numerical investigation of the influence of IRS on one of the localized solutions of the CCQGLE, namely, the stable stationary pulses. The basic CCQGLE of this paper [see Eq. (1)], which describes the propagation of ultrashort optical pulses under the effect of IRS in the presence of linear and nonlinear gain as well as spectral filtering, is the model applied earlier in [22]. Our aim is to examine numerically the influence of IRS on the stable stationary pulses in the presence of constant linear and nonlinear gain as well as spectral filtering. We have found that a small change of the value of the parameter γ leads to qualitatively different behavior of the evolution of pulse amplitudes. We prove that the strong dependence of the latter on the parameter γ is related to the existence of the Poincaré-Andronov-Hopf bifurcation and the appearance of the unstable limit cycle, which completely explains our numerical findings.

The paper is organized as follows. The physical meaning and applications of the generalized CCQGLE are presented in Sec. II. The numerical results suggesting a strong dependence on the parameter γ are presented in Sec. III. In Sec. IV a nonlinear system of ordinary differential equations (ODEs) is introduced by means of the method of conserved quantities. In Sec. V we apply the bifurcation analysis to the nonlinear system of ODEs. In Sec. VI we apply the results of the analysis from Sec. V in order to establish the existence of the Poincaré-Andronov-Hopf bifurcation and the appearance of the unstable limit cycle. The agreement between theory and numerical results is discussed in Sec. VII. We summarize in Sec. VIII.

II. BASIC EQUATION

The propagation of ultrashort pulses in the presence of spectral filtering, linear and nonlinear gain/loss, and IRS is

*Corresponding author: ivan_uzunov@tu-sofia.bg
†zhdgeorg@tu-sofia.bg
‡tna@tu-sofia.bg

described by the generalized CCQGLE [22]

$$i\frac{\partial U}{\partial x}+\frac{1}{2}\frac{\partial^2 U}{\partial t^2}+|U|^2U = i\delta U+i\beta\frac{\partial^2 U}{\partial t^2}+i\varepsilon|U|^2U+i\mu|U|^4U+\gamma U\frac{\partial}{\partial t}(|U|^2), \tag{1}$$

where U is the normalized envelope of the electric field, x is the normalized propagation distance, t is the retarded time, δ is the linear gain or loss coefficient, β describes spectral filtering (gain dispersion), ε is related to the nonlinear gain-absorption process, and μ, if negative, accounts for the saturation of the nonlinear gain. The last term in Eq. (1) describes IRS, an important nonlinear physical effect that has to be taken into account when femtosecond optical pulses propagate in optical fibers. It is related to the first moment of the nonlinear response function (the slope of the Raman gain spectrum) and leads to different physical phenomena such as the soliton self-frequency shift and breakup of the N-soliton bound states (for a review see [18–20]).

Equation (1) has been used to model the solution of the problem of linear-wave growth in bandwidth-limited amplified soliton transmission systems [3,4]. In the context of solid state lasers, Eq. (1) ($\mu=\gamma=0$) was proposed as a master equation for a fast saturable absorber and additive pulse mode locking [5] and later was used ($\gamma=0$) as a model for self-limited additive pulse mode locking [26]. It turned out that Eq. (1) ($\mu=\gamma=0$) was also applicable as a master equation for the mode-locked fiber lasers [27]. In addition, the all-normal-dispersion passively-mode-locked fiber lasers were successfully described by means of Eq. (1) ($\gamma=0$) [28–30]. Generally, the CCQGLE ($\gamma=0$) has proved to be a good model for the real mode-locked lasers (for a review see [31–33]).

III. NUMERICAL RESULTS

As a result of intensive numerical investigation of the CCQGLE, some areas in the space of physical parameters δ, β, ε, and μ have been established in which stable localized solutions of the CCQGLE exist [34,14,22]. It is believed that if $\delta<0$, $\beta>0$, and $\mu<0$ the background instability is avoided [34,14,22]. Our calculations confirm these results, so we use parameters that satisfy these conditions.

The numerical results for the solution of Eq. (1) presented here have been obtained by means of the fourth-order Runge-Kutta method in the interaction picture (RK4IP). The RK4IP can generally be interpreted as the exponential Runge-Kutta method applied to the solution of a parabolic partial differential equation [35–39]. The method is with a fourth-order convergence, which makes it a good alternative to the all-known variants of the split-step Fourier method (SSFM). Moreover, in some cases, the method is significantly more accurate than the SSFM [36,37,39]. A comparison of performances of the RK4IP and SSFM has been made for a number of cases and a perfect match has been obtained. To verify our numerical model, we have compared our results with those of [24,40] obtained by means of the SSFM. Excellent agreement has been established. The numerical parameters applied for the numerical results presented here are the sampling rate 8192–16 384, the numerical time window 81.92–655.36, and the propagation step 0.001. PRODUCT ORIGIN 8.5 has been applied for the calculation of the average values of amplitudes and frequencies**.**

As a representative example of our results we set the parameters $\delta=-0.02$, $\beta=0.05$, $\varepsilon=0.1$, and $\mu=-0.02$ and give the following values of γ: $\gamma=0.054\,083\,3, 0.064\,083\,3, 0.074\,083\,3$ (The choice of these values of γ will become clear in Secs. V and VI). Equation (1) has been solved with the initial condition $U(0,t)=\eta_0\mathrm{sech}(\eta_0 t)\exp(-ik_0 t)$, where η_0 and k_0 are the initial amplitude and initial frequency, respectively. The results obtained for the evolution of pulse amplitudes during the propagation are presented in Fig. 1.

Figure 1(a) shows numerically the appearance of a stable stationary pulse with the average values of amplitude $\bar{\eta}=1.412$ and frequency $\bar{k}=-0.866$. The results shown in Fig. 1(a) have been extended by the numerical solution of Eq. (1) with the same form of the initial condition but with initial amplitudes in the range $\eta_0\subset(1.043–2.037)$ and the same initial frequency $k_0=-0.8$. In all cases behavior similar to that shown in Fig. 1(a) has been observed, namely, after some transition period in x the average values of $\bar{\eta}$and $\bar{k}$ asymptotically go to $\bar{\eta}=1.412$ and $\bar{k}=-0.866$. (Note that larger values of $x_{\max}$ up to 500 have been used without a qualitative change of the results presented.) Thus, it is clear that there is a stable attractor in the phase space of Eq. (1).

Figure 1(b) shows the unstable pulsating solution with average values of the amplitude $\bar{\eta}=1.248$ and frequency $\bar{k}=-0.801$. Figure 1(c) numerically presents the pulse destruction.

Comparing these three cases we clearly see that the small change of the value of the parameter γ leads to qualitatively different behavior of the evolution of pulse amplitudes. In fact, under the increased value of γ we obtain the plain pulsating solution. Note that in some respect this result is just the opposite of the results reported in [24,25], where the higher-order effects were found to transform the localized pulsating solutions in fixed-shape solutions for some range of parameter values. Such a strong dependence on the parameter γ suggests the idea of a bifurcation dependence of γ. In what follows we will prove the bifurcation type of the discussed dependence and describe it qualitatively.

IV. DERIVATION OF THE ODE SYSTEM

For the analysis of Eq. (1) we apply the adiabatic perturbation method described in [18]. Considering terms on the right-hand side of Eq. (1) of a small value, we can find its solution as a perturbed soliton solution of the nonlinear Schrödinger equation (NLSE) in the form

$$U(x,t)=\eta(x)\mathrm{sech}\{\eta(x)[t-\tau(x)]\}\exp\{-ik(x)t+i\sigma(x)\}, \tag{2}$$

where $\eta(x)$ and $k(x)$ are, respectively, the soliton amplitude and frequency [18]. In addition, $d[\tau(x)]/dx=-k$ and $d[\sigma(x)]/dx=\frac{1}{2}(\eta^2-\kappa^2)$ are the pulse position and pulse phase, respectively. Applying the adiabatic perturbation

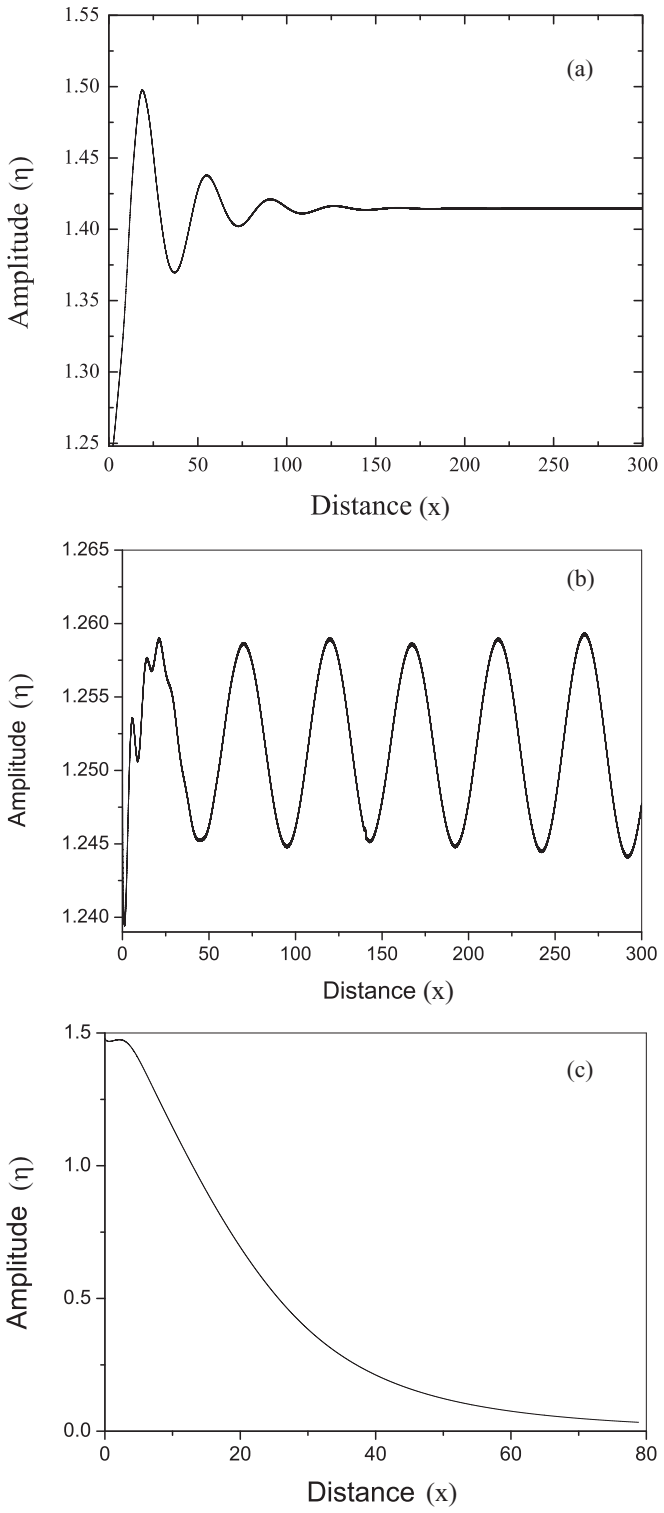

FIG. 1. Evolution of the pulse amplitude $\eta(x)$ with distance according to Eq. (1) with $\delta = -0.02$, $\beta = 0.05$, $\varepsilon = 0.1$, and $\mu = -0.02$ for (a) $\gamma = 0.054\,083\,3$ and $x_{\max} = 300$, with initial conditions $\eta_0 = 1.25$ and $k_0 = -0.8$; (b) $\gamma = 0.064\,083\,3$, $x_{\max} = 300$ with initial conditions $\eta_0 = 1.25$ and $k_0 = -0.8$; and (c) $\gamma = 0.074\,083\,3$, $x_{\max} = 80$ with initial conditions $\eta_0 = 1.48$ and $k_0 = -0.8$.

method, we derive the equations for the evolution of the first two conserved quantities of the NLSE [18], namely, the total energy and the momentum (or the mean frequency), i.e.,

$$C_1 = \int_{-\infty}^{+\infty} |U(x,t)|^2 dt,$$

$$C_2 = \frac{i}{2}\int_{-\infty}^{+\infty}\left(U(x,t)\frac{\partial U^*(x,t)}{\partial t} - U^*(x,t)\frac{\partial U(x,t)}{\partial t}\right)dt,$$

with x. Using the expressions of the conserved quantities through the soliton amplitude and soliton frequency [18], we obtain the following system of ODEs to describe the evolution of the soliton amplitude and frequency:

$$\begin{aligned}\frac{d\eta}{dx} &= 2\delta\eta + \frac{2}{3}(2\varepsilon - \beta)\eta^3 - 2\beta\eta k^2 + \frac{16}{15}\mu\eta^5,\\ \frac{dk}{dx} &= -\frac{4}{3}\beta k\eta^2 - \frac{8}{15}\gamma\eta^4.\end{aligned} \tag{3}$$

The system of ODEs (3) was derived by means of a perturbed inverse scattering method [18] in [22]. It has the equilibrium points

$$(\eta_{\rm EP}, k_{\rm EP}) = \left(\eta_{\rm EP}, -\frac{2\gamma}{5\beta}\eta_{\rm EP}^2\right) \tag{4a}$$

where

$$\begin{aligned}\eta_{\rm EP} &= \sqrt{A \pm \sqrt{A^2 - B}},\\ k_{\rm EP} &= -\frac{2\gamma}{5\beta}\eta_{\rm EP}^2 = -\frac{2\gamma}{5\beta}[A \pm \sqrt{A^2 - B}],\end{aligned} \tag{4b}$$

$$\begin{aligned}A &= \frac{25\beta(\beta - 2\varepsilon)}{80\beta\mu - 24\gamma^2},\\ B &= \frac{75\delta\beta}{40\beta\mu - 12\gamma^2}.\end{aligned} \tag{4c}$$

Depending on the values of A and B, there are two steady-state solutions if

$$A > \sqrt{B} > 0 \quad \text{[case (i)]} \tag{5a}$$

and one steady-state solution if

$$\begin{aligned}&B < 0 && \text{[case (ii)]},\\ &A = \sqrt{B} > 0 && \text{[case (iii)]},\\ &B = 0, \quad A > 0 && \text{[case (iv)]}.\end{aligned} \tag{5b}$$

As we study the system of ODEs (3) for $\delta < 0$, $\beta > 0$, and $\mu < 0$ and all of them are different from zero, cases (ii) and (iv) are excluded from our consideration. Moreover, as we look for the bifurcation behavior with respect to parameter γ for fixed values of δ, β, ε, and μ, case (iii) should also be excluded. Finally, in this work we will focus only on case (i).

V. BIFURCATION ANALYSIS OF THE ODE SYSTEM

In this section we analyze the behavior of the ODE system (3). Its behavior determines the solution of the initial wave equation (1). The system (3) depends on a large number of parameters having a different range of variation. In further analysis we will focus our attention on the parameter γ, which is related to the effect of IRS. The presented results are obtained using the Poincaré-Andronov-Hopf bifurcation analysis [41–43], wherein γ is regarded as a bifurcation parameter.

We find the Jacobian matrix of the ODE system (3):

$$\mathbf{J} = \begin{bmatrix} 2\delta + 2(2\varepsilon - \beta)\eta^2 - 2\beta k^2 + \frac{16}{3}\mu\eta^4 & -4\beta\,\eta\,k \\ -\frac{8}{3}\beta\,\eta\,k - \frac{32}{15}\gamma\,\eta^3 & -\frac{4}{3}\beta\eta^2 \end{bmatrix}. \tag{6}$$

The eigenvalues of the matrix $\mathbf{J}$ are determined by the characteristic equation

$$p_{\mathbf{A}}(\lambda) = \lambda^2 - (\mathrm{tr}\mathbf{J})\,\lambda + \det\mathbf{J} = 0. \tag{7}$$

It is well known that a Poincaré-Andronov-Hopf bifurcation arises in the case of complex conjugate eigenvalues. Having this in mind, we can write the roots of Eq. (7) (or the eigenvalues of the matrix $\mathbf{J}$) in the following way:

$$\lambda_{1,2} = \tfrac{1}{2}\mathrm{tr}\mathbf{J} \pm i\,\tfrac{1}{2}\sqrt{-\Delta} = \alpha(\gamma) \pm i\beta(\gamma), \tag{8}$$

where

$$\Delta = \Delta(\gamma) = (\mathrm{tr}\mathbf{J})^2 - 4\det\mathbf{J}. \tag{9}$$

After long but straightforward computation we find

$$\alpha(\gamma) = \frac{1}{2}\mathrm{tr}\mathbf{J} = \delta + \left(2\varepsilon - \frac{5}{3}\beta\right)\eta_{\mathrm{EP}}^2 + \left(\frac{8}{3}\mu - \frac{4}{25}\frac{\gamma^2}{\beta}\right)\eta_{\mathrm{EP}}^4, \tag{10}$$

$$\beta(\gamma) = \frac{1}{2}\sqrt{-\Delta} = \frac{1}{2}\sqrt{\frac{512}{75}\gamma^2\eta_{\mathrm{EP}}^6 - \left[2\delta + 2\left(2\varepsilon - \frac{1}{3}\beta\right)\eta_{\mathrm{EP}}^2 + \left(\frac{16}{3}\mu - \frac{8}{25}\frac{\gamma^2}{\beta}\right)\eta_{\mathrm{EP}}^4\right]^2}, \tag{11}$$

$$\alpha'(\gamma) = \frac{d\alpha(\gamma)}{d\gamma} = \left(2\varepsilon - \frac{5}{3}\beta\right)\frac{d(\eta_{\mathrm{EP}}^2)}{d\gamma} + \left(\frac{16}{3}\mu - \frac{8}{25}\frac{\gamma^2}{\beta}\right)\eta_{\mathrm{EP}}^2\frac{d\,(\eta_{\mathrm{EP}}^2)}{d\gamma} - \frac{8}{25}\frac{\gamma}{\beta}\eta_{\mathrm{EP}}^4, \tag{12}$$

where

$$\frac{d\left(\eta_{\mathrm{EP}}^2\right)}{d\gamma} = A' \pm \frac{2AA' - B'}{2\sqrt{A^2 - B}},$$

$$A' = \frac{dA}{d\gamma} = \frac{75\beta\gamma(\beta - 2\varepsilon)}{4(10\beta\mu - 3\gamma^2)^2},$$

$$B' = \frac{dB}{d\gamma} = \frac{225\beta\gamma\delta}{2(10\beta\mu - 3\gamma^2)^2}.$$

The expressions for Δ, $\alpha(\gamma)$, $\beta(\gamma)$, and $\alpha'(\gamma)$ given here depend on all parameters, but we assume that they are functions of the parameter γ, as we want to study the dynamics of the system (3) where the parameter γ varies. These expressions, as well as the expressions for the equilibrium points, contain the quantity η_{EP}. The subscript EP means that the corresponding quantity is calculated for a given equilibrium point, which has not been concretized until now. Note that in case (i), which is defined by Eq. (5a), the quantity η_{EP} accepts two values η_{EP}^+ and η_{EP}^-, which correspond to the plus and minus signs, respectively, in Eq. (4b). Hence, the system (3) has two equilibrium points.

From the Poincaré-Andronov-Hopf bifurcation theory it follows that the system (3) possesses a limit cycle only in the case where the parameter γ takes the value γ_0, for which the following nonhyperbolicity condition (conjugate pair of imaginary eigenvalues) and transversality condition (the eigenvalues cross the imaginary axis with nonzero speed) are satisfied, i.e.,

$$\alpha(\gamma_0) = 0, \quad \Delta(\gamma_0) < 0, \quad \alpha'(\gamma_0) \neq 0. \tag{13}$$

To find the value of γ_0 we first choose an equilibrium point that satisfies Eq. (5a) or case (i). Then we take the plus sign in the formulas for η_{EP} and k_{EP} given in Eq. (4b). The resulting expressions for η_{EP} and k_{EP} are imported into Eqs. (10)–(12). The function $\alpha = \alpha(\gamma)$ given by Eqs. (10), (4a), and (4b) defines a complicated (irrational one) dependence of α on the parameter γ (more precisely on γ^2). In fact, α could take the real and complex values. Depending on the fixed values of δ, β, ε, and μ, the first of Eqs. (13) does not always have a solution. Thus, fixing the parameters δ, β, ε, and μ, we could only build numerically the graphs $\alpha = \alpha(\gamma)$ and $\Delta = \Delta(\gamma)$ for some range of variation of γ in which $\alpha = \alpha(\gamma)$ and $\Delta = \Delta(\gamma)$ are real functions and a solution for γ_0 exists. In Fig. 2 we present the graphs of $\alpha = \alpha(\gamma)$ and $\Delta = \Delta(\gamma)$ for the following values of the parameters: $\delta = -0.02$, $\beta = 0.05$, $\varepsilon = 0.1$, and $\mu = -0.02$ in the range of variation of $\gamma \subset [0, 0.08]$. As we can see, $\alpha = \alpha(\gamma)$ passes through zero at $\gamma_0 = 0.064\,083\,3$, while $\Delta = \Delta(\gamma)$ at this point is negative. For the value $\gamma_0 = 0.064\,083\,3$ the derivative $\alpha'(\gamma_0) = 2.7358$ is different from zero. Thus, $\gamma_0 = 0.064\,083\,3$ turns out to be the bifurcation value of the parameter γ for the Poincaré-Andronov-Hopf bifurcation.

If the system (3) allows a limit cycle, it is important to determine the stability of this limit cycle. The Poincaré-Andronov-Hopf bifurcation theory gives an analytical expression that aids in the determination of the stability of the arising limit cycle. To obtain this expression it is necessary to put the system

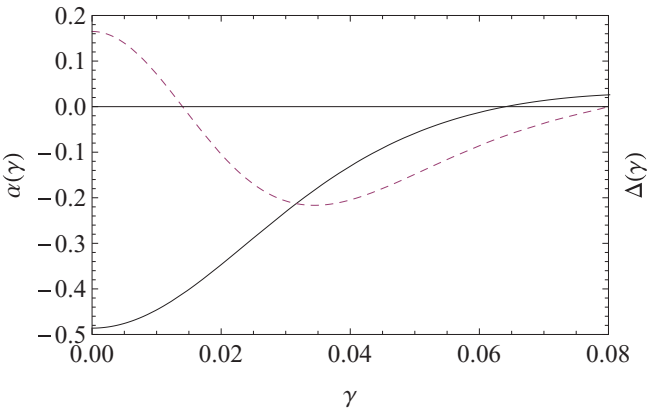

FIG. 2. (Color online) Graphs of $\alpha = \alpha(\gamma)$ (solid line) and $\Delta = \Delta(\gamma)$ (dashed line).

(3) into a normal form. We do not describe this process; it is shown in detail in [39]. We briefly describe the first two steps, which represent the so-called center manifold reduction of the system (3). First, we transform the regarded equilibrium point of the system (3) to the origin. Then we perform a linear transformation of the coordinates so that the linear part of the system is put into a canonical Jordan form. After these operations the system (3) takes the form

$$\begin{bmatrix}\dot{p}\\ \dot{q}\end{bmatrix} = \begin{bmatrix}f(p,q,\gamma)\\ g(p,q,\gamma)\end{bmatrix} = \begin{bmatrix}\alpha(\gamma) & -\beta(\gamma)\\ \beta(\gamma) & \alpha(\gamma)\end{bmatrix}\begin{bmatrix}p\\ q\end{bmatrix} + \begin{bmatrix}f_1(p,q,\gamma)\\ g_1(p,q,\gamma)\end{bmatrix}. \quad (14)$$

Taking into account the last system, we define the quantity

$$a = \frac{1}{16}(f_{ppp} + f_{pqq} + g_{ppq} + g_{qqq}) + \frac{1}{16\omega}[f_{pq}(f_{pp} + f_{qq}) - g_{pq}(g_{pp} + g_{qq}) - f_{pp}g_{pp} + f_{qq}g_{qq}], \quad (15)$$

where $\omega = \beta(\gamma_0)$ and the values of the derivatives are evaluated in the bifurcation point of the system (14), which is $(p,q,\gamma) = (0\,,0\,,\gamma_0)$. Now we can state that the system (3) admits a limit cycle in the case where not only conditions (13) are satisfied, but the so-called genericity condition is also fulfilled, i.e., $a \neq 0$. Moreover, when $a < 0$ the limit cycle is stable and when $a > 0$ it is unstable. Finally, we note that in Eq. (15) we can take the derivatives of the functions f_1 and g_1 instead of the derivatives of the functions f and g. This information is sufficient to analyze the system (3) with respect to the Poincaré-Andronov-Hopf bifurcation theory.

VI. NUMERICAL ANALYSIS OF THE ODE SYSTEM

Let us now study the ODE system (3) numerically by means of a computer software system Wolfram *Mathematica* 8.0. Remember that in all cases it is assumed that $\delta = -0.02$, $\beta = 0.05$, $\varepsilon = 0.1$, and $\mu = -0.02$. The numerical study of this system includes two groups of results. In the first case, we numerically build the phase portraits of the system (3) where the parameter γ takes the values below, at, and above the bifurcation value $\gamma_0 = 0.064\,083\,3$. The second group of results includes the numerical solution of the system (3) for the cases considered in Fig. 1.

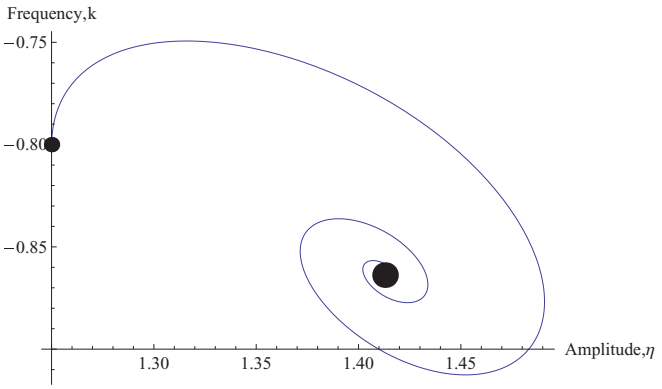

FIG. 3. (Color online) Phase portrait of the ODE system (3) for $\delta = -0.02$, $\beta = 0.05$, $\varepsilon = 0.1$, $\mu = -0.02$, $\gamma = 0.054\,083\,3$, and initial conditions $\eta_0 = 1.25$ and $k_0 = -0.8$ (marked with a small circle) for $x_{\max} = 500$, demonstrating the existence of the stable focal point (marked with a large circle).

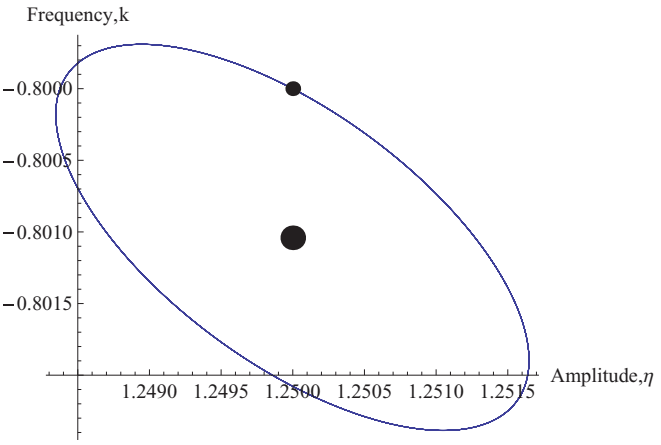

FIG. 4. (Color online) Phase portrait of the system of ODEs (3) for $\delta = -0.02$, $\beta = 0.05$, $\varepsilon = 0.1$, $\mu = -0.02$, $\gamma = 0.064\,083\,3$, and initial conditions $\eta_0 = 1.25$ and $k_0 = -0.8$ (marked with a small circle) for $x_{\max} = 500$, demonstrating the appearance of the limit cycle. The fixed point is marked with a large circle.

Case 1. The value of γ is below the bifurcation value $\gamma = 0.054\,083\,3 < \gamma_0$. Here $A = 1.248\,33$ and $B = 0.998\,668$. The fixed point $(\eta_{\rm EP}, k_{\rm EP}) = (1.412\,96\,, -0.863\,796)$ is a stable focal point. The corresponding phase portrait is shown in Fig. 3.

Case 2. The value of γ is equal to the bifurcation value $\gamma = 0.064\,083\,3 = \gamma_0$. Here $A = 1.050\,07$ and $B = 0.840\,054$. The fixed point is $(\eta_{\rm EP}, k_{\rm EP}) = (1.25\,, -0.801\,041)$. The corresponding phase portrait is shown in Fig. 4.

Further, we have calculated the expected period of the limit cycle. As $\beta(\gamma_0) = 0.126\,037$, we expect the period to be $T \approx 2\pi/\beta(\gamma_0) \approx 49.8518$. The quantity $a = 0.001\,826\,24$ is positive, so we expect that the observed limit cycle is an unstable one. This expectation has been proved by studying

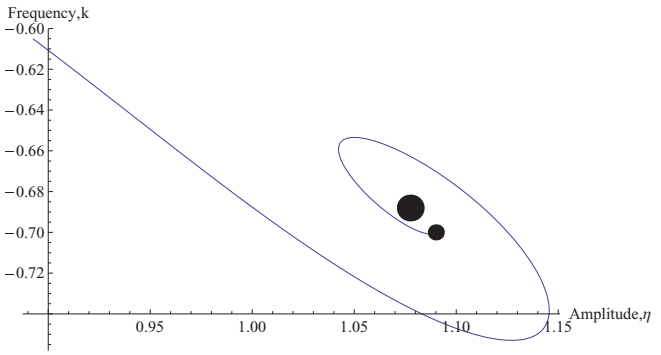

FIG. 5. (Color online) Phase portrait of the ODE system (3) for $\delta = -0.02$, $\beta = 0.05$, $\varepsilon = 0.1$, $\mu = -0.02$, $\gamma = 0.074\,083\,3$, and initial conditions $\eta_0 = 1.09$ and $k_0 = -0.7$ (marked with a small circle) for $x_{\max} = 120$, demonstrating the existence of unstable focal point (marked with a large circle).

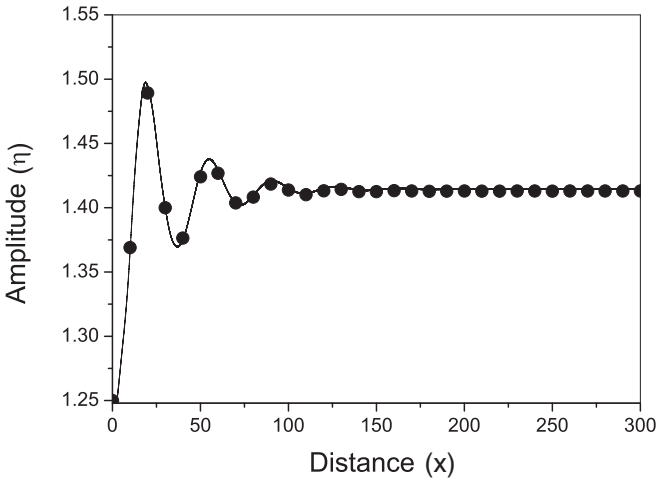

FIG. 6. Evolution of the pulse amplitude $\eta(x)$ with $\delta = -0.02$, $\beta = 0.05$, $\varepsilon = 0.1$, and $\mu = -0.02$ for $\gamma = 0.054\,083\,3$ and $x_{\max} = 300$, with initial conditions $\eta_0 = 1.25$ and $k_0 = -0.8$. The solid line denotes the numerical solution of the CCQGLE (1) and the circles denote the numerical solution of the ODE system (3).

the phase portrait for different values of the initial amplitude and velocity.

Case 3. The value of γ is above the bifurcation value $\gamma = 0.074\,083\,3 > \gamma_0$. Here $A = 0.885\,603$ and $B = 0.708\,483$. The fixed point $(\eta_{EP}, k_{EP}) = (1.077\,47\,, -0.688\,051)$ is an unstable focal point. The corresponding phase portrait is shown in Fig. 5.

The considered increase of the value of the parameter γ ($\gamma = 0.054\,083\,3$, $0.064\,083\,3$, and $0.074\,083\,3$) describes the typical bifurcation behavior of the ODE system (3) regarding this parameter. We start with the stable focal point with $\gamma = 0.054\,083\,3$. By increasing the value of γ we arrive at the bifurcation value $\gamma_0 = 0.064\,083\,3$. According to the Poincaré-Andronov-Hopf bifurcation theory, an unstable limit cycle emerges. A further increase of γ to $\gamma = 0.074\,083\,3$ leads us to an unstable focal point.

The second group of results includes the numerical solution of the ODE system (3) for the cases considered in Fig. 1. In Fig. 6 we compare the results in Fig. 1(a) for the evolution of the pulse amplitude $\eta(x)$ with the results obtained by the numerical solution of the CCQGLE (1).

Moreover, the ODE system (3) with the initial amplitudes in the range $\eta_0 \subset (1.045$–$2.036)$ and initial frequency $k_0 = -0.8$ has been solved and the results have been compared with the results obtained by the numerical solution of the CCGLE (1). Very good agreement of the results obtained by the two methods has been established (as in Fig. 6). We can conclude that these results clearly indicate the applicability of the ODE system (3) for the description of Eq. (1) with the assumed values of the parameters δ, β, ε, and μ.

VII. DISCUSSION

After showing the applicability of the ODE system (3) for the description of numerical solutions of the Eq. (1), we now discuss the results of Sec. III in view of the bifurcation analysis performed in Secs. IV–VI. For the value of γ smaller than the critical one $\gamma = 0.054\,083\,3 < \gamma_0$, Fig. 1(a) presents numerically the appearance of a stable stationary pulse with average values of the amplitude $\bar{\eta} = 1.412$ and frequency $\bar{k} = -0.866$. These values for the average quantities coincide nicely with the values for the stable focal fixed point $\eta_{EP} = 1.412\,96$ and $k_{EP} = -0.863\,796$, obtained in Sec. VI (case 1).

For the bifurcation value of $\gamma = 0.064\,083\,3 = \gamma_0$, Fig. 1(b) shows the unstable pulsating pulse propagation with average values of amplitude $\bar{\eta} = 1.248$ and frequency $\bar{k} = -0.801$. These values could be compared to the values of the fixed point $\eta_{EP} = 1.25$ and $k_{EP} = -0.801\,041$ related to the appearance of the unstable limit cycle discussed in Sec. VI (case 2). We mention the very similar results for the period of the amplitude fluctuation numerically observed in Fig. 1(b) and the one calculated in Sec. VI (case 2).

For the value of γ larger than the critical one $\gamma = 0.074\,083\,3 > \gamma_0$, Fig. 1(c) presents numerically destruction of the pulse. Such behavior could be expected in view of the unstable focal point obtained in Sec. VI (case 3).

We conclude that with the assumed values of the parameters δ, β,ε, and μ the performed bifurcation analysis of the ODE system (3) in Secs. IV–VI reveals and clarifies the observed numerical solutions of Eq. (1).

VIII. CONCLUSION

We have numerically examined the influence of IRS on the stable stationary pulses in the presence of constant linear and nonlinear gain as well as spectral filtering. The numerical results have shown that a small change of the value of the parameter γ leads to qualitatively different behavior of the evolution of pulse amplitudes. In particular, it has been established that if γ is increased, the transition from a stable stationary pulse to a plane pulsating solution is observed. Using the first two conserved quantities of the NLSE, we have derived the ODE system (3). The bifurcation analysis of the ODE system (3) has proved that the strong dependence of the pulse dynamics on the parameter γ is related to the existence of the Poincaré-Andronov-Hopf bifurcation and the appearance of an unstable limit cycle.

An interesting question remains for further analysis. Are there regions in the parametric space for which stable limit cycles appear? A similar question for an equation slightly different from Eq. (1) was recently studied in [44,45].

[1] M. C. Cross and P. C. Hohenberg, Rev. Mod. Phys. **65**, 851 (1993).

[2] I. S. Aranson and L. Kramer, Rev. Mod. Phys. **74**, 99 (2002).

[3] M. Matsumoto, H. Ikeda, T. Uda, and A. Hasegawa, J. Lightwave Technol. **13**, 658 (1995).

[4] Y. Kodama, M. Romagnoli, and S. Wabnitz, Electron. Lett. **28**, 1981 (1992).

[5] H. A. Haus, J. G. Fujimoto, and E. P. Ippen, J. Opt. Soc. Am. B **8**, 2068 (1991).
[6] F. X. Kärtner, J. Ausder Au, and U. Keller, IEEE J. Sel. Top. Quantum Electron. **4**, 159 (1998).
[7] N. R. Pereira and L. Stenflo, Phys. Fluids **20**, 1733 (1977).
[8] P.-A. Bélanger, L. Gagnon, and C. Pare, Opt. Lett. **14**, 943 (1989).
[9] R. Conte and M. Musette, Pure Appl. Opt. **4**, 315 (1995).
[10] R. Conte and M. Musette, in *Dissipative Solitons*, edited by N. Akhmediev and A. Ankievicz, Lecture Notes in Physics Vol. 661 (Springer, Berlin, 2005).
[11] N. N. Akhmediev and A. Ankiewicz, *Solitons, Nonlinear Pulses and Beams* (Chapman and Hall, London, 1997).
[12] J. M. Soto-Crespo, N. Akhmediev, and A. Ankiewicz, Phys. Rev. Lett. **85**, 2937 (2000).
[13] W. Chang, A. Ankiewicz, N. N. Akhmediev and J. M. Soto-Crespo, Phys. Rev. E **76**, 016607 (2007).
[14] N. N. Akhmediev, J. M. Soto-Crespo, and G. Town, Phys. Rev. E **63**, 056602 (2001).
[15] N. N. Akhmediev and A. Ankiewicz, in *Dissipative Solitons* (Ref. [10]).
[16] S. C. Mancas and S. R. Choudhury, Chaos Solitons Fractals **40**, 91 (2009).
[17] S. C. Mancas and S. R. Choudhury, Theor. Math. Phys. **152**, 1160 (2007).
[18] A. Hasegawa and Y. Kodama, *Solitons in Optical Communications* (Clarendon, Oxford, 1995).
[19] G. P. Agrawal, *Nonlinear Fiber Optics*, 3rd ed. (Academic, San Diego, 2001).
[20] G. P. Agrawal, *Applications of Nonlinear Fiber Optics* (Academic, San Diego, 2001).
[21] P.-A. Bélanger, Opt. Express **14**, 12174 (2006).
[22] S. C. V. Latas and M. F. S. Ferreira, Opt. Commun. **251**, 415 (2005).
[23] Z. Li, L. Li, H. Tian, G. Zhou, and K. H. Spatschek, Phys. Rev. Lett. **89**, 263901 (2002).
[24] S. C. V. Latas, M. F. S. Ferreira, and M. V. Facao, Appl. Phys. B **104**, 131 (2011).
[25] S. C. V. Latas and M. F. S. Ferreira, Opt. Lett. **37**, 3897 (2012).
[26] F. I. Khatri, J. D. Moores, G. Lenz, and H. A. Haus, Opt. Commun. **114**, 447 (1995).
[27] L. E. Nelson, D. J. Jones, K. Tamura, H. A. Haus, and E. P. Ippen, Appl. Phys. B **65**, 277 (1997).
[28] W. H. Renninger, A. Chong, and F. W. Wise, Phys. Rev. A **77**, 023814 (2008).
[29] F. W. Wise, A. Chong, and W. H. Renninger, Laser Photon. Rev. **2**, 58 (2008).
[30] W. H. Renninger, A. Chong, and F. W. Wise, Opt. Express **19**, 22496 (2011).
[31] J. Nathan Kutz, SIAM Rev. **48**, 629 (2006).
[32] P. Grelu and N. N. Akhmediev, Nat. Photon. **6**, 84 (2012).
[33] E. Ding, W. H. Renninger, F. W. Wise, P. Grelu, E. Shilizerman, and J. Nathan Kutz, Int. J. Opt. **2012**, 354156 (2012).
[34] J. M. Soto-Crespo, N. N. Akhmediev, and V. V. Afanasjev, J. Opt. Soc. Am. B **13**, 1439 (1996).
[35] B. M. Caradoc-Davies, Ph.D. thesis, University of Otago, 2000.
[36] J. Hult, J. Lightwave Technol. **25**, 3770 (2007).
[37] A. Heidt, J. Lightwave Technol. **27**, 3984 (2009).
[38] Z. Zhang, L. Chen, and X. Bao, Opt. Express **18**, 8261 (2010).
[39] S. Balac, A. Fernandez, F. Mane, F. Mehats, and R. Texier-Picard, http://hal.inria.fr/hal-00850518, version 1-7 (HAL-Inria, Rocquencourt, 2013).
[40] I. M. Uzunov and T. N. Arabadzhiev, Phys. Rev. E **84**, 026607 (2011).
[41] S. Wiggins, *Introduction to Applied Nonlinear Dynamical Systems*, 2nd ed. (Springer, New York, 2003).
[42] Yu. Kuznetsov, *Elements of Applied Bifurcation Theory*, 2nd ed. (Springer, New York, 1998).
[43] M. Han and P. Yu, Normal, *Forms, Melnikov Functions and Bifurcations of Limit Cycles* (Springer, London, 2012).
[44] I. M. Uzunov and Zh. D. Georgiev, Proceedings of Tenth International Conference on Computational Methods in Science and Engineering, Athens, 2014 (unpublished).
[45] I. M. Uzunov and Zh. D. Georgiev, Journal of Computational Methods in Physics (2014) (to be published).